1. General materials, methods and equipment

Chemicals: All chemicals were purchased from established vendors (e.g. Sigma-Aldrich, Acros Organics, Glen Research) and used without purification unless otherwise noted. Optima grade acetonitrile was obtained from Fisher Scientific and degassed under vacuum prior to HPLC purification. All reactions to prepare various phosphormidites were carried out in round bottom flasks and stirred with Teflon®-coated magnetic stir bars under inert atmosphere when needed. Analytical thin layer chromatography (TLC) was performed using EMD 250 micron flexible aluminum backed, UV F_{254} pre-coated silica gel plates and visualized under UV light (254 nm) or by staining with phosphomolybdic acid, ninhydrin or anisaldehyde. Reaction solvents were removed by a Büchi rotary evaporator equipped with a dry ice-acetone condenser. Analytic and preparative HPLC was carried out on an Agilent 1220 Infinity HPLC with diode array detector. Concentration and lyophilization of aqueous samples were performed using Savant Sc210A SpeedVac Concentrator (Thermo), followed by Labconco Freeze-Dryer system.

Proton nuclear magnetic resonance spectra (1H NMR) were recorded on Bruker Ultrashield^{TM} Plus 600/500/400/300 MHz instruments at 24 ^{o}C. Chemical shifts of ^{1}H and ^{13}C NMR spectra are reported as d in units of parts per million (ppm) relative to tetramethylsilane (d 0.0) or residual solvent signals: chloroform-d (d 7.26, singlet), methanol-d_4 (d 3.30, quintet), and deuterium oxide-d_2 (d 4.80, singlet). Coupling constants are expressed in Hz. Mass spectra were collected at the UPITT MASSSPEC lab on a Q-Exactive^{TM} Thermo Scientific LC-MS with electron spray ionization (ESI) probe.

2. Supplementary figures

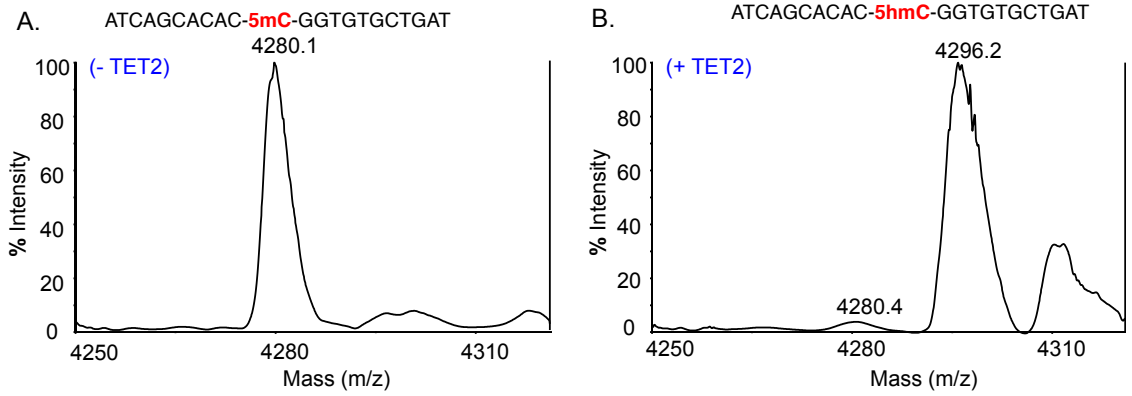

Supplementary Figure S1: (A) MALDI MS spectra of synthetized 22-nucleotide TET2 substrate containing 5mC. The upper strand is identical to its palindromic complementary strand. (B) TET2-mediated full conversion of 5mC to 5hmC in 22-nt substrate.

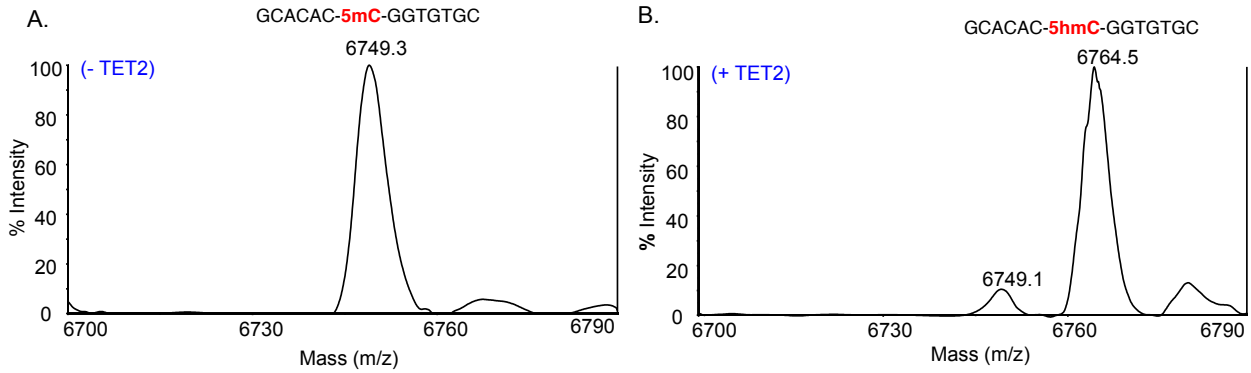

Supplementary Figure S2: (A) MALDI MS spectra of synthetized 14-nucleotide TET2 substrate containing 5mC. The upper strand is identical to its palindromic complementary strand. (B) TET2-mediated full conversion of 5mC to 5hmC in 14-nt substrate.

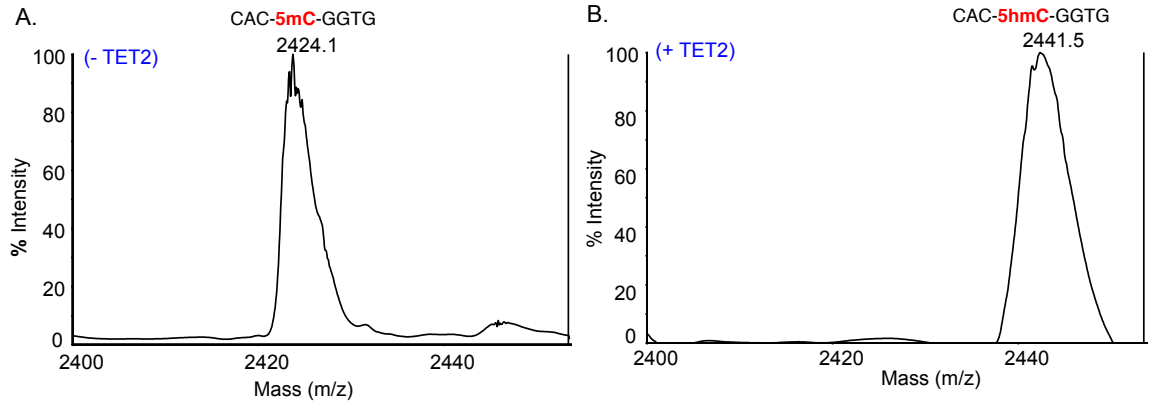

Supplementary Figure S3: (A) MALDI MS spectra of synthetized 8-nucleotide TET2 substrate containing 5mC. The upper strand is identical to its palindromic complementary strand. (B) TET2-mediated full conversion of 5mC to 5hmC in 8-nt substrate.

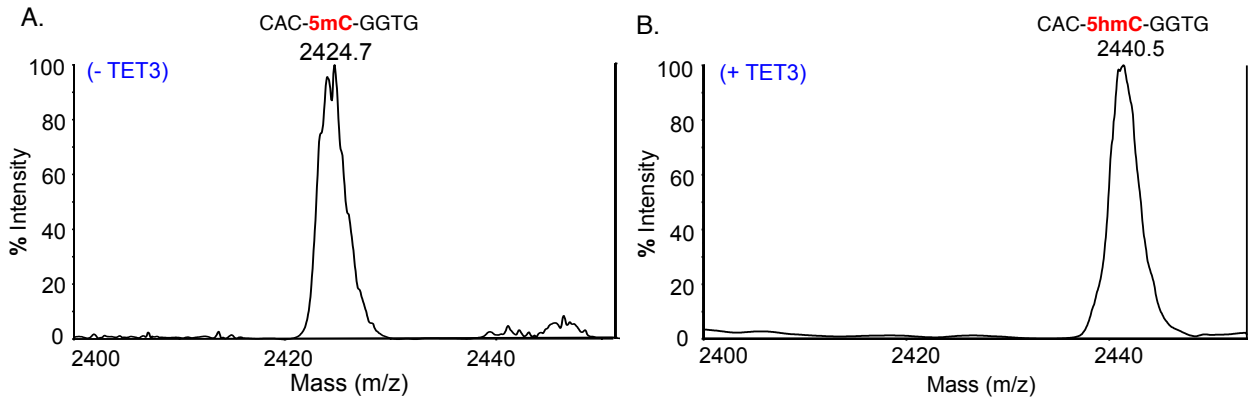

Supplementary Figure S4: (A) MALDI MS spectra of synthetized 8-nucleotide substrate containing 5mC. The upper strand is identical to its palindromic complementary strand. (B) TET3-mediated full conversion of 5mC to 5hmC in 8-nt substrate.

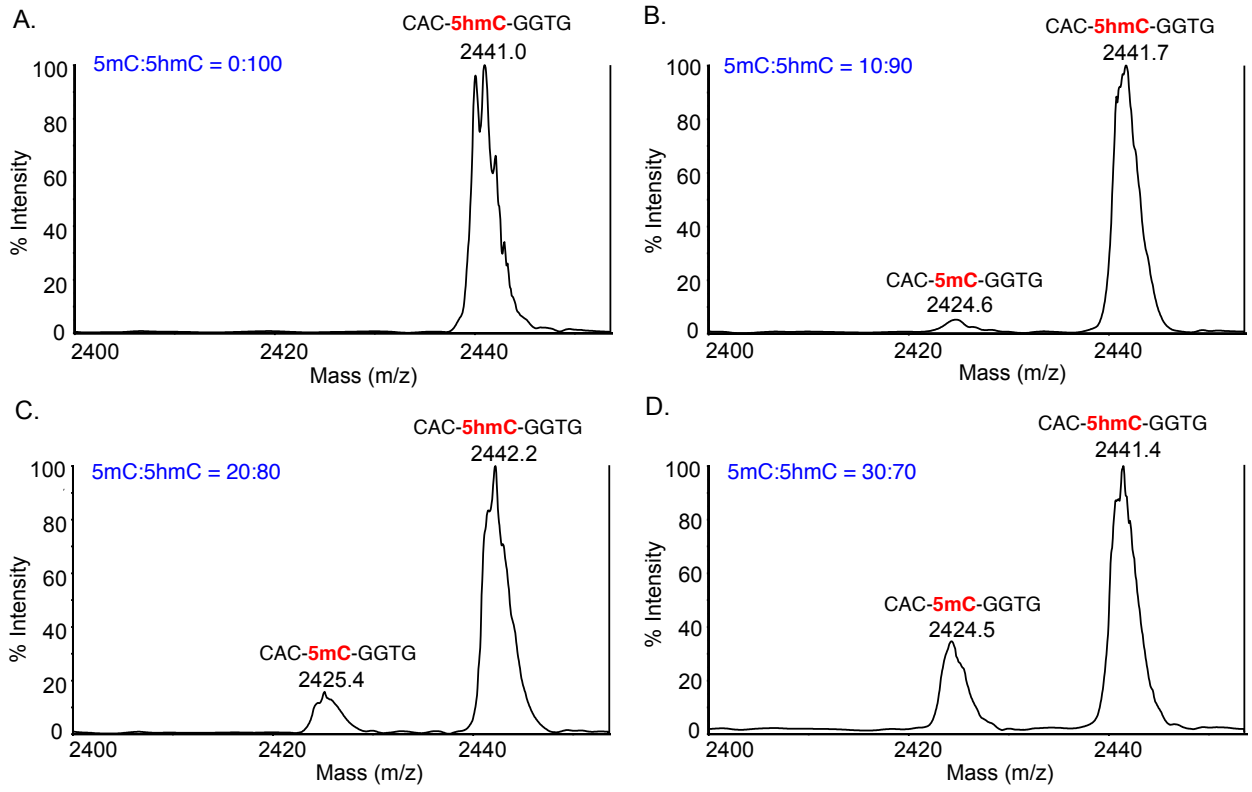

Supplementary Figure S5: (A-D) MALDI MS spectra of synthetized 8-nucleotide DNAs containing 5mC and 5hmC in different ratios.

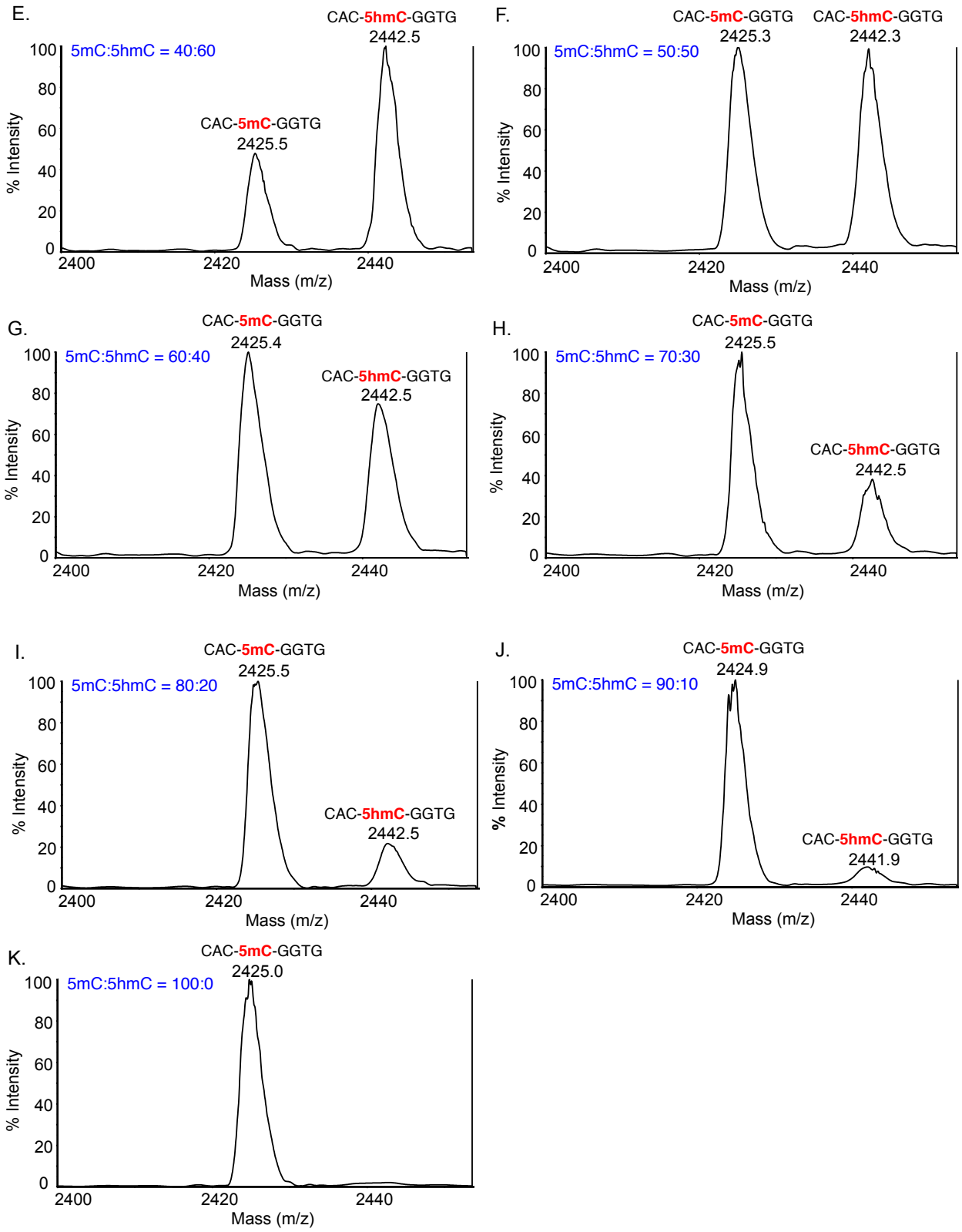

Supplementary Figure S5 continued: (E-K) MALDI MS spectra of synthetized 8-nucleotide DNAs containing 5mC and 5hmC in different ratios.

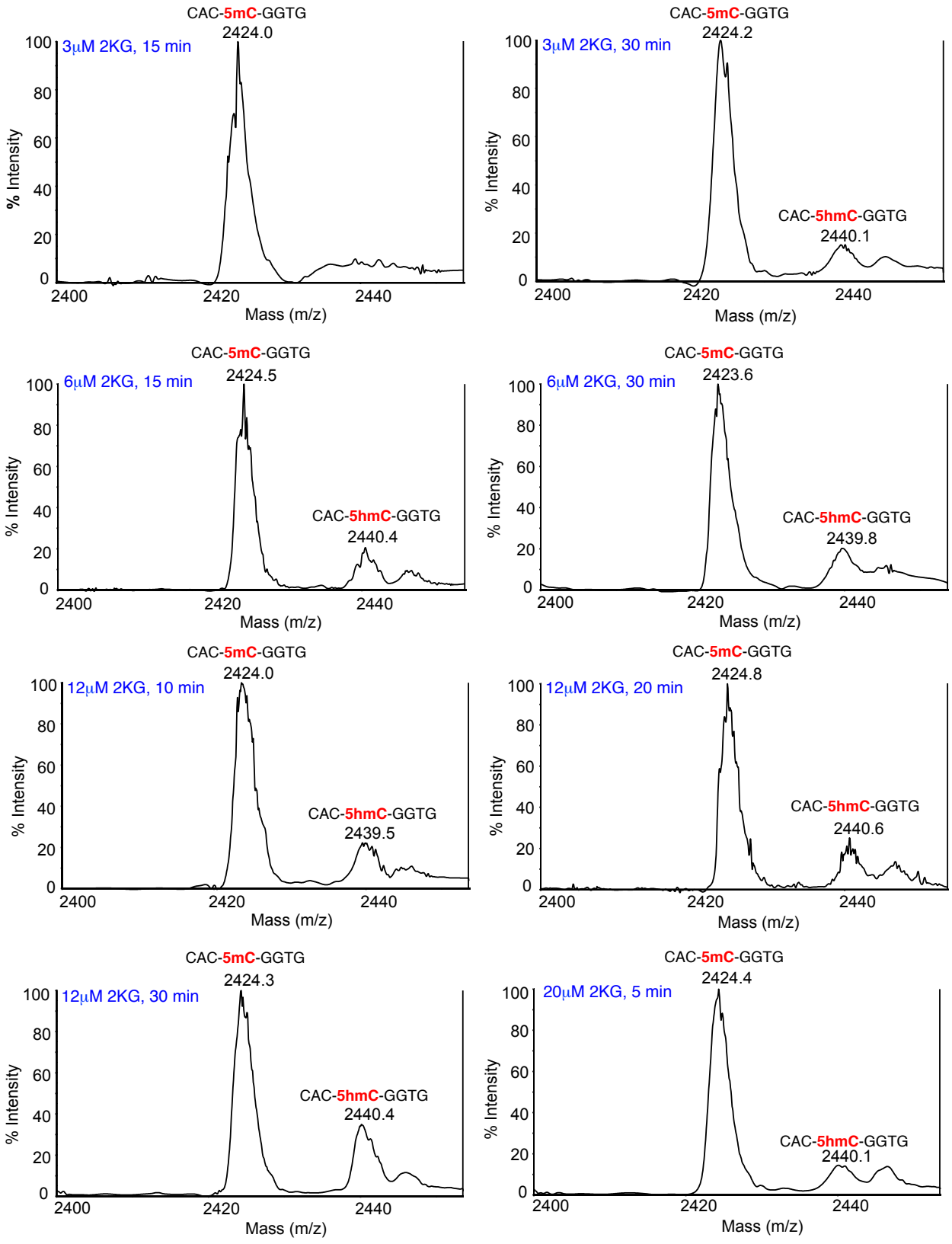

Supplementary Figure S6: 2KG concentration- and time-dependent catalytic activity of TET2

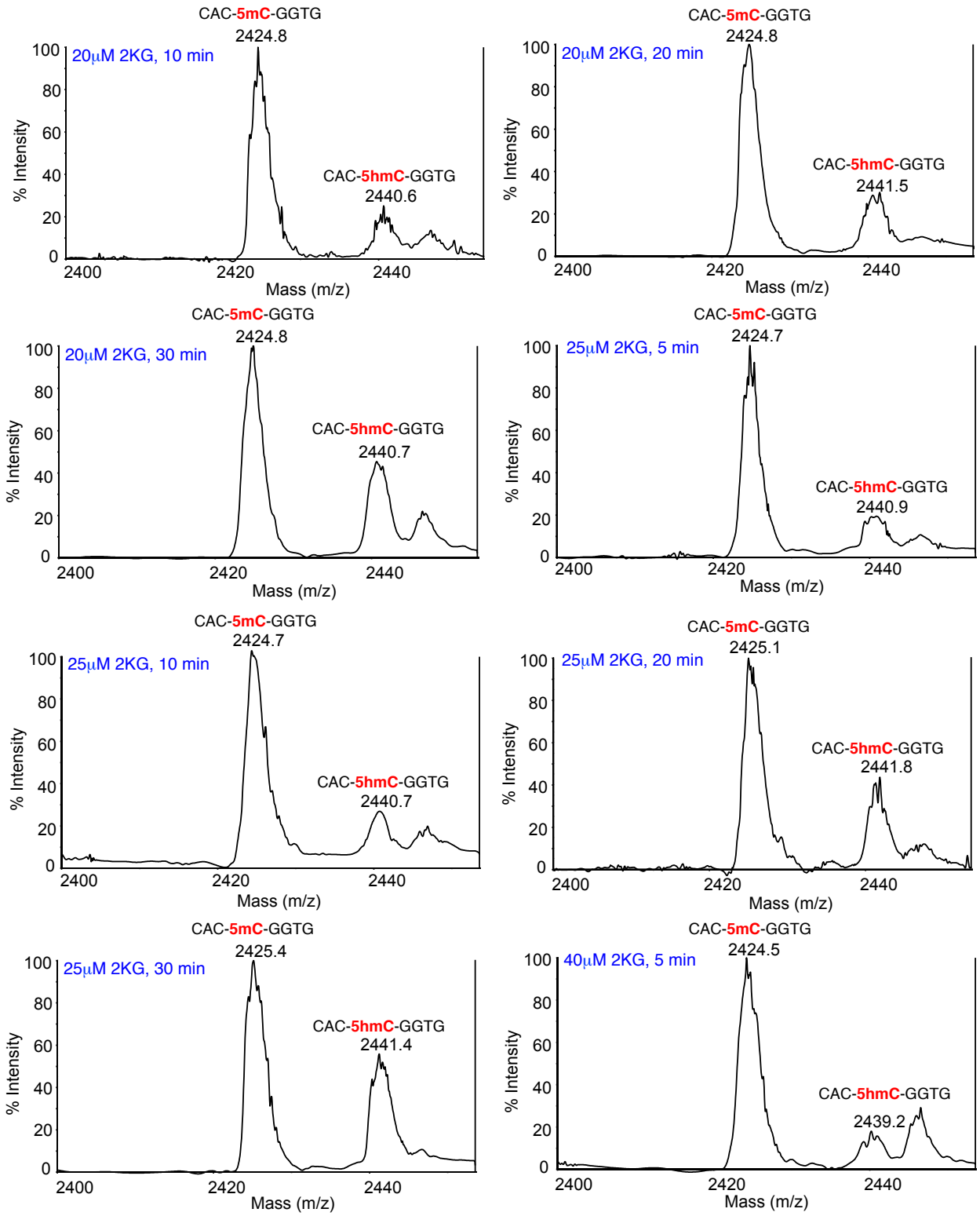

Supplementary Figure S6 continued: 2KG concentration- and time-dependent catalytic activity of TET2

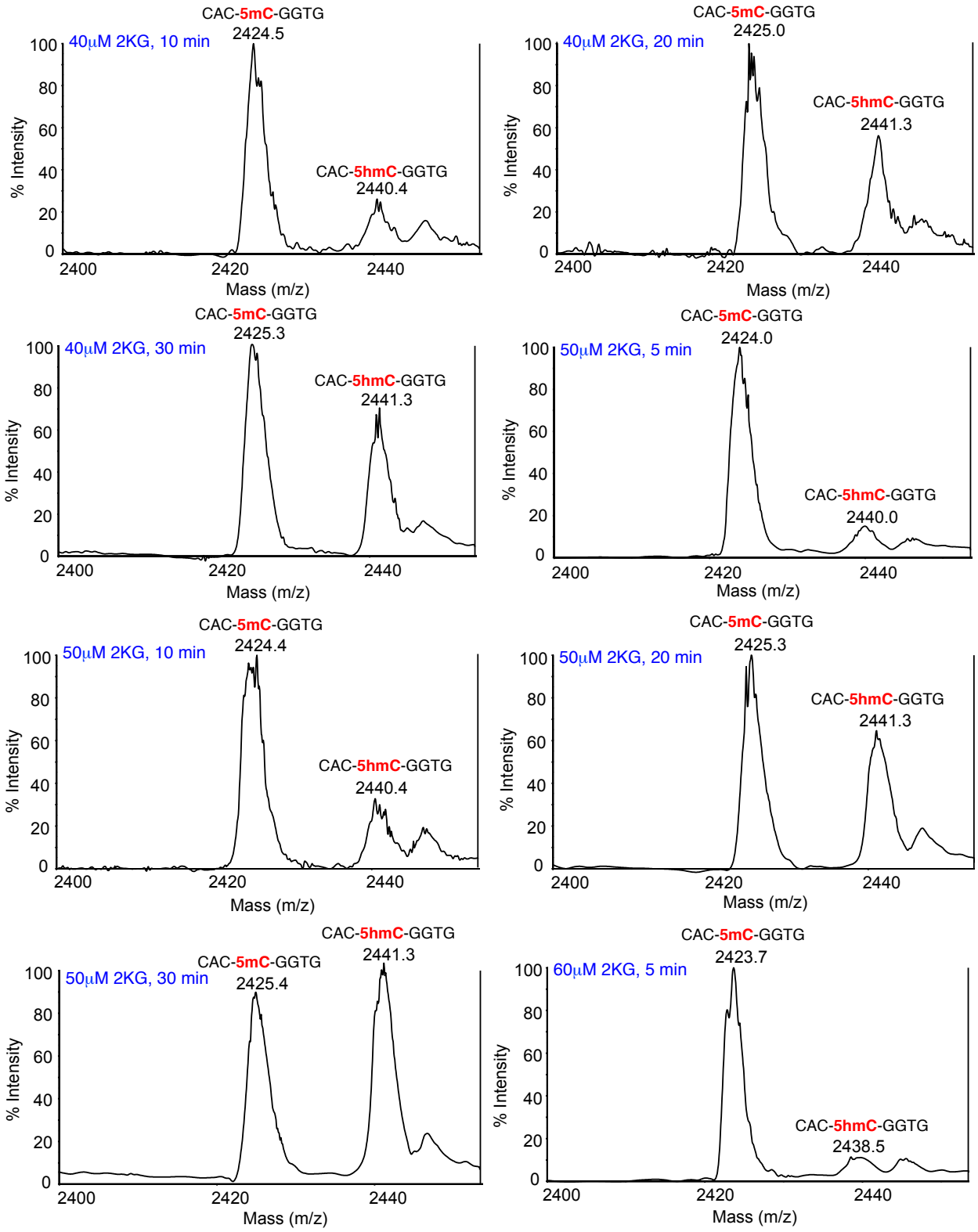

Supplementary Figure S6 continued: 2KG concentration- and time-dependent catalytic activity of TET2

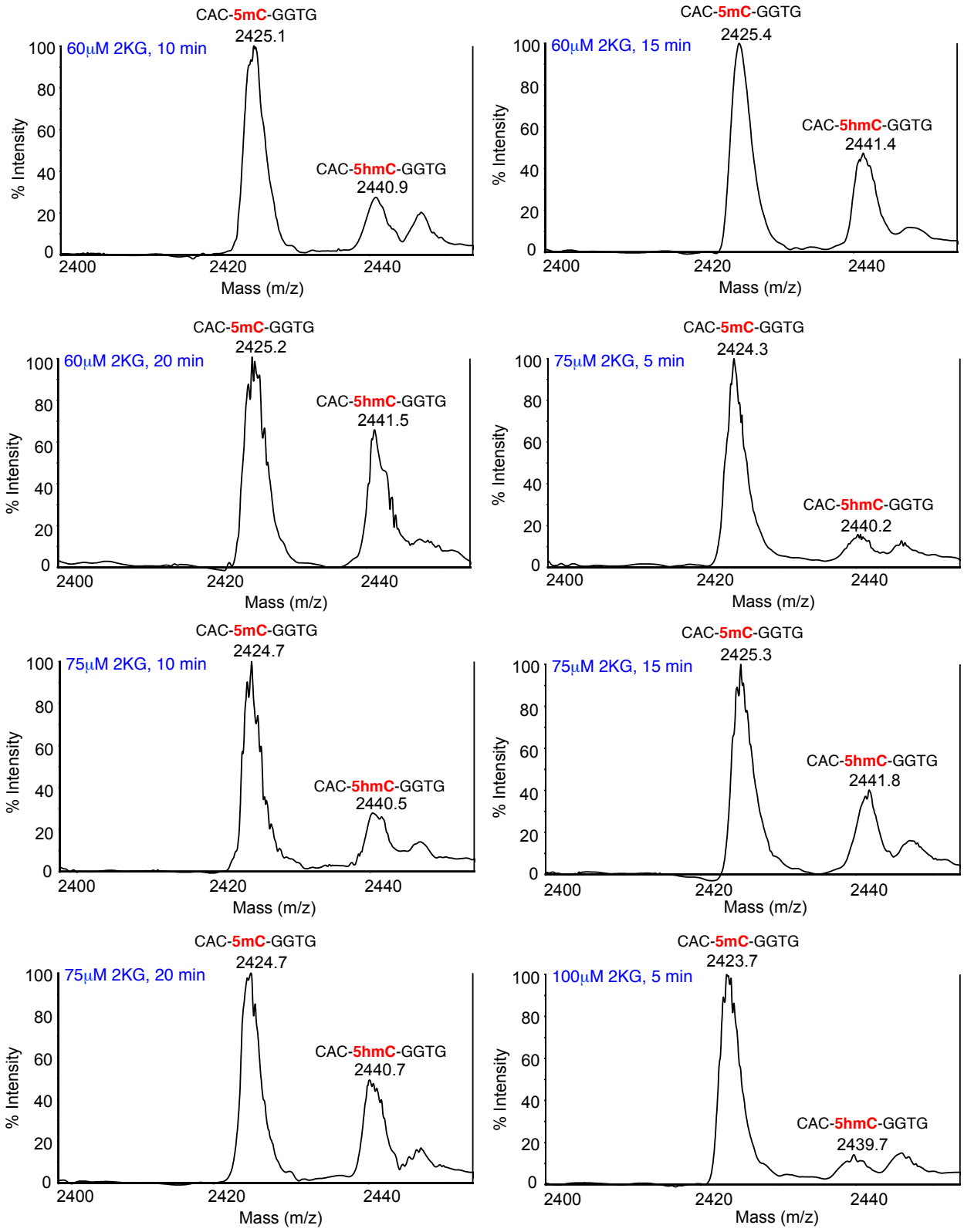

Supplementary Figure S6 continued: 2KG concentration- and time-dependent catalytic activity of TET2

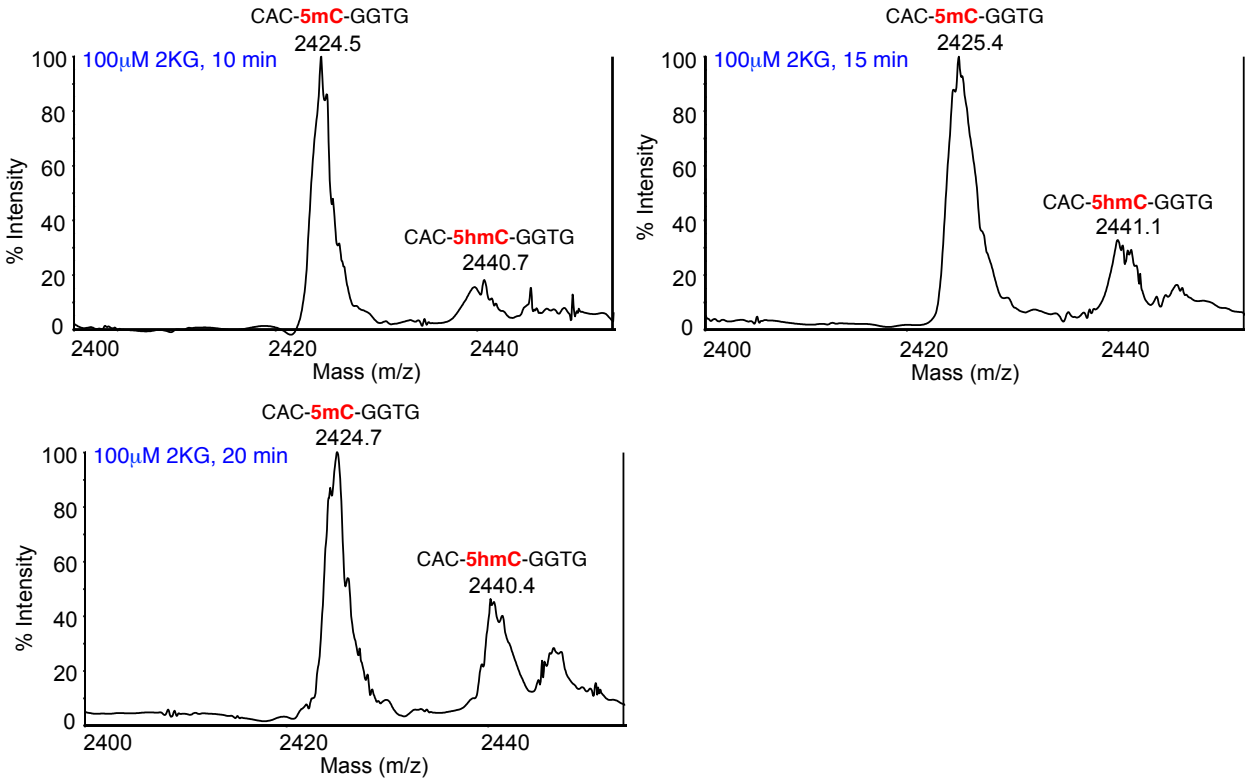

Supplementary Figure S6 continued: 2KG concentration- and time-dependent catalytic activity of TET2

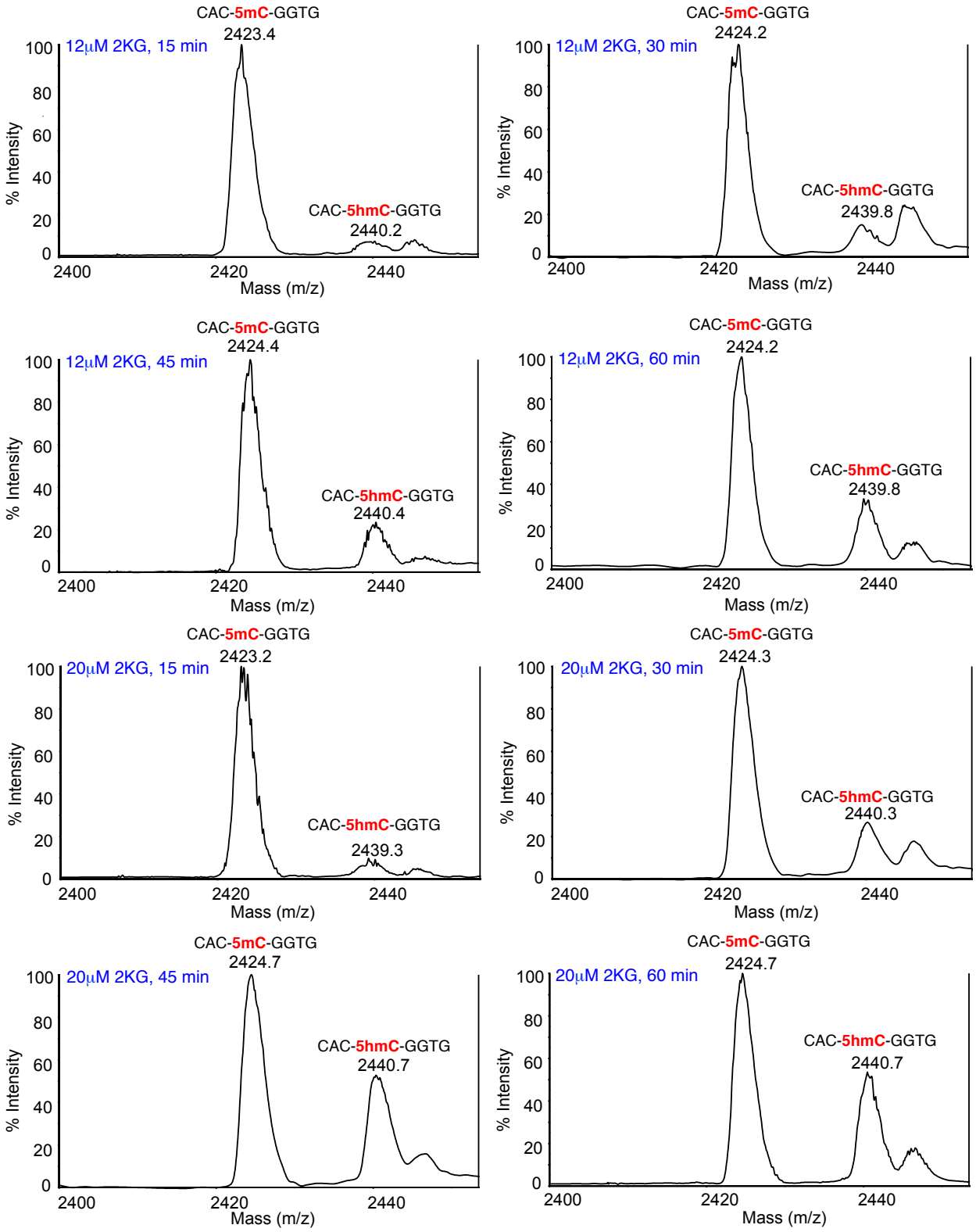

Supplementary Figure S7: 2KG concentration- and time-dependent catalytic activity of TET3

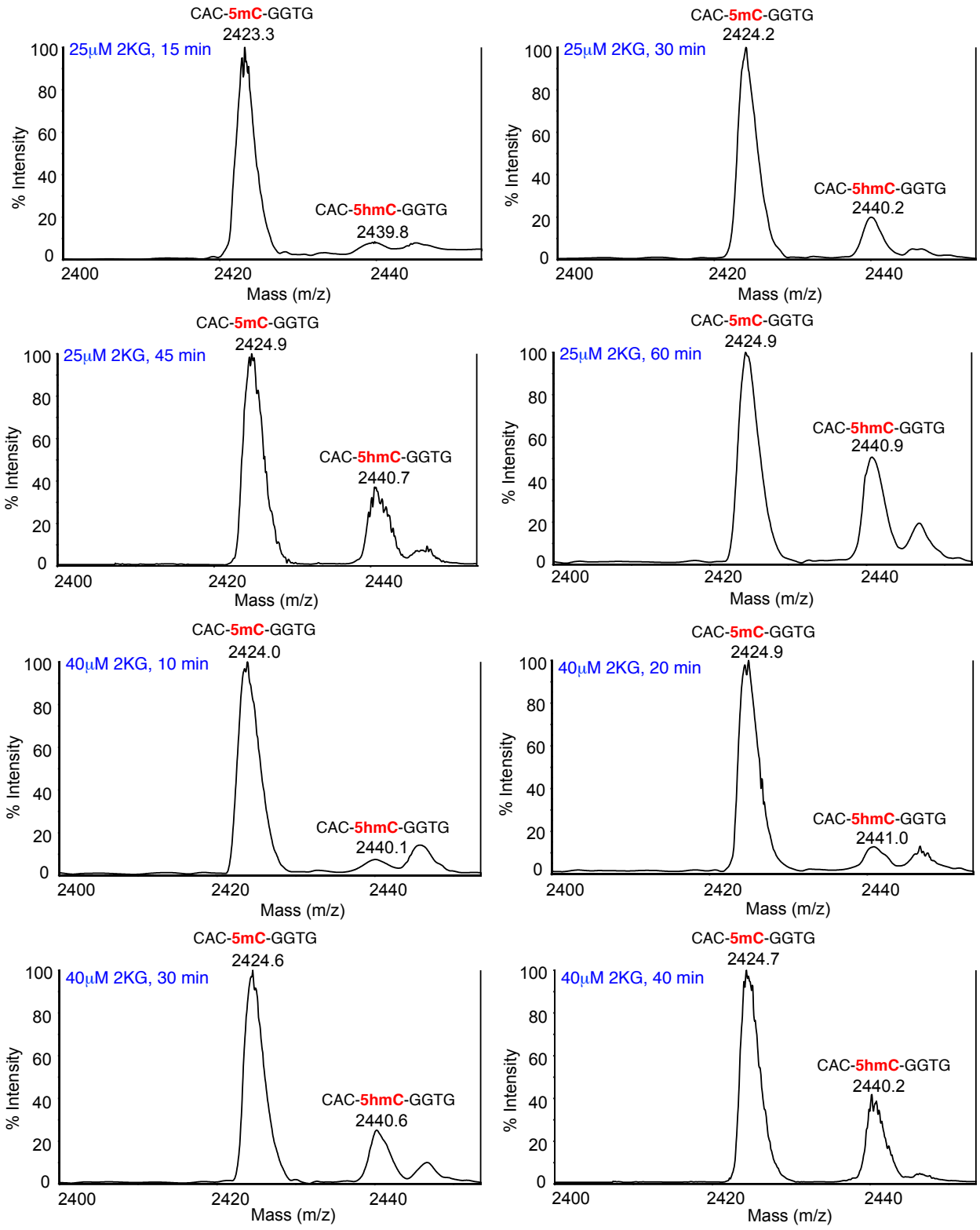

Supplementary Figure S7 continued: 2KG concentration- and time-dependent catalytic activity of TET3

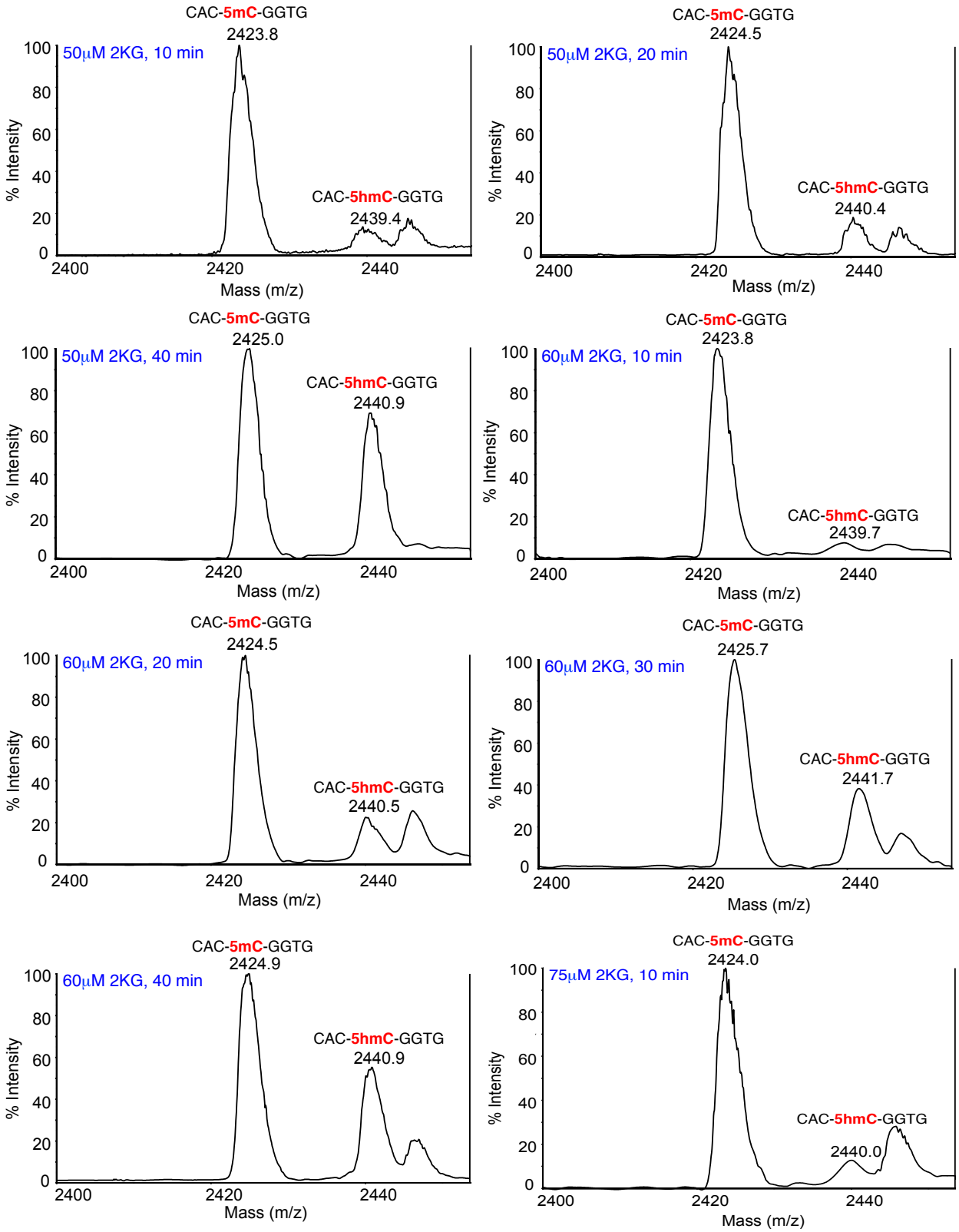

Supplementary Figure S7 continued: 2KG concentration- and time-dependent catalytic activity of TET3

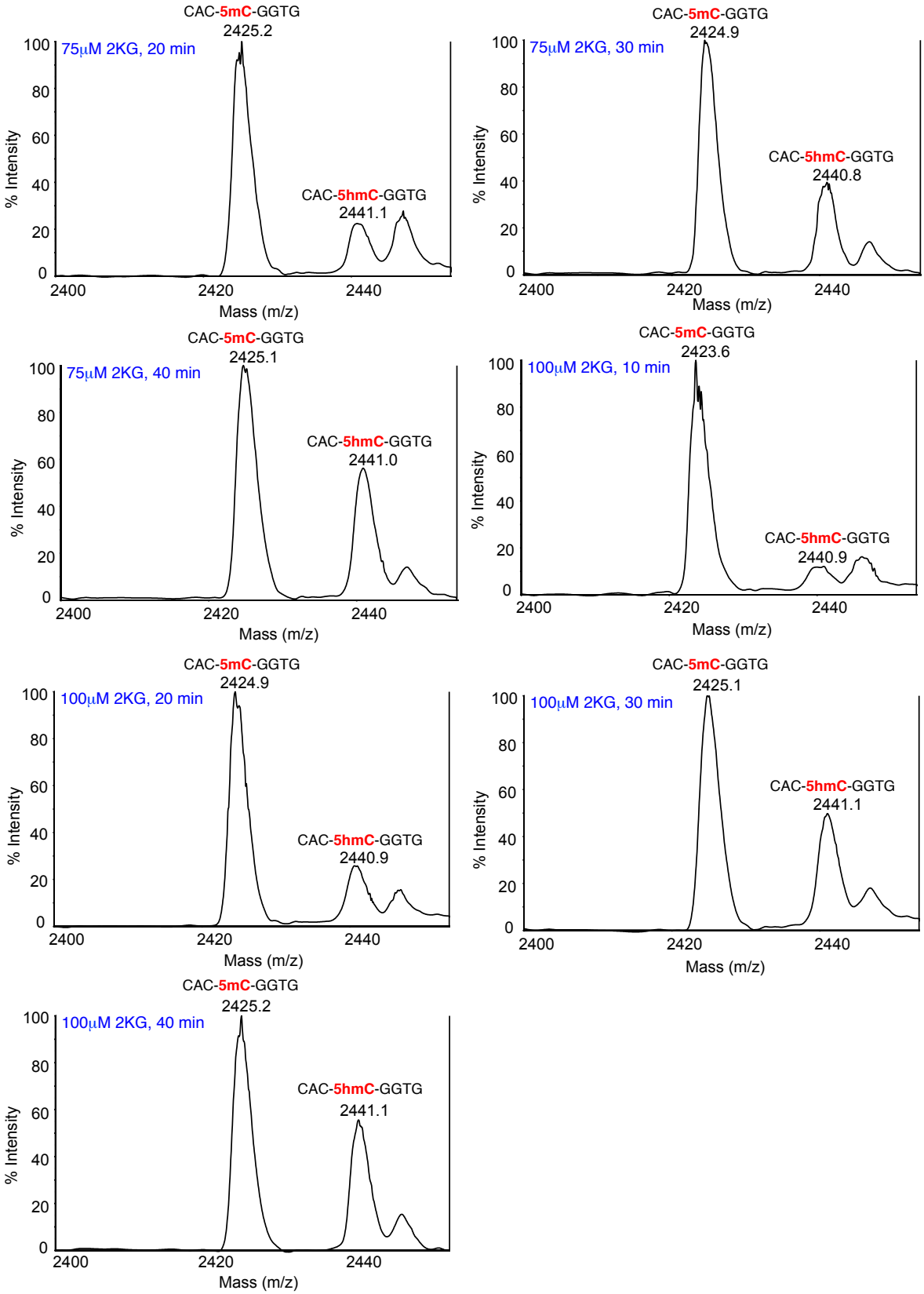

Supplementary Figure S7 continued: 2KG concentration- and time-dependent catalytic activity of TET3

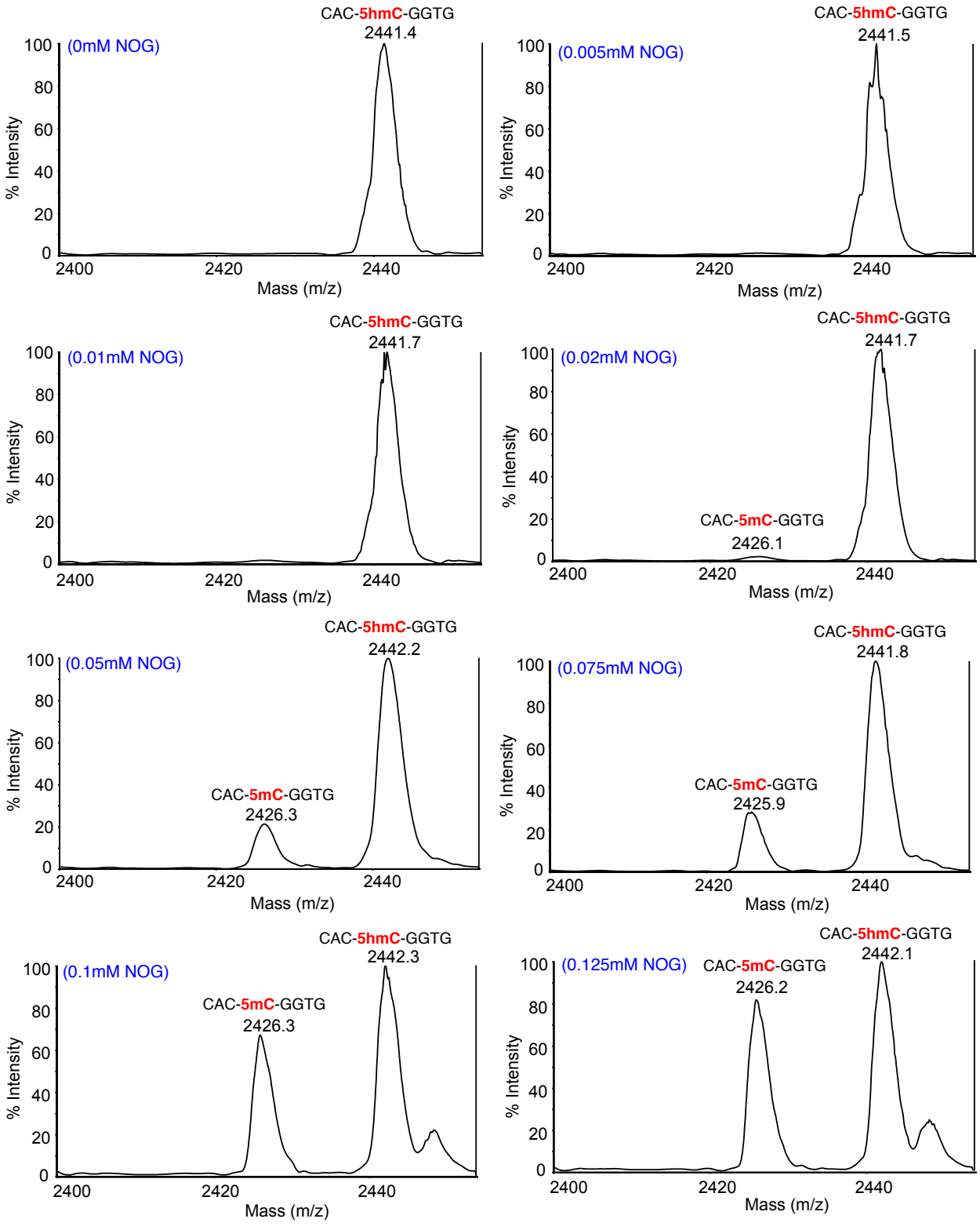

Supplementary Figure S8: NOG concentration-dependent inhibition of TET2 catalytic activity

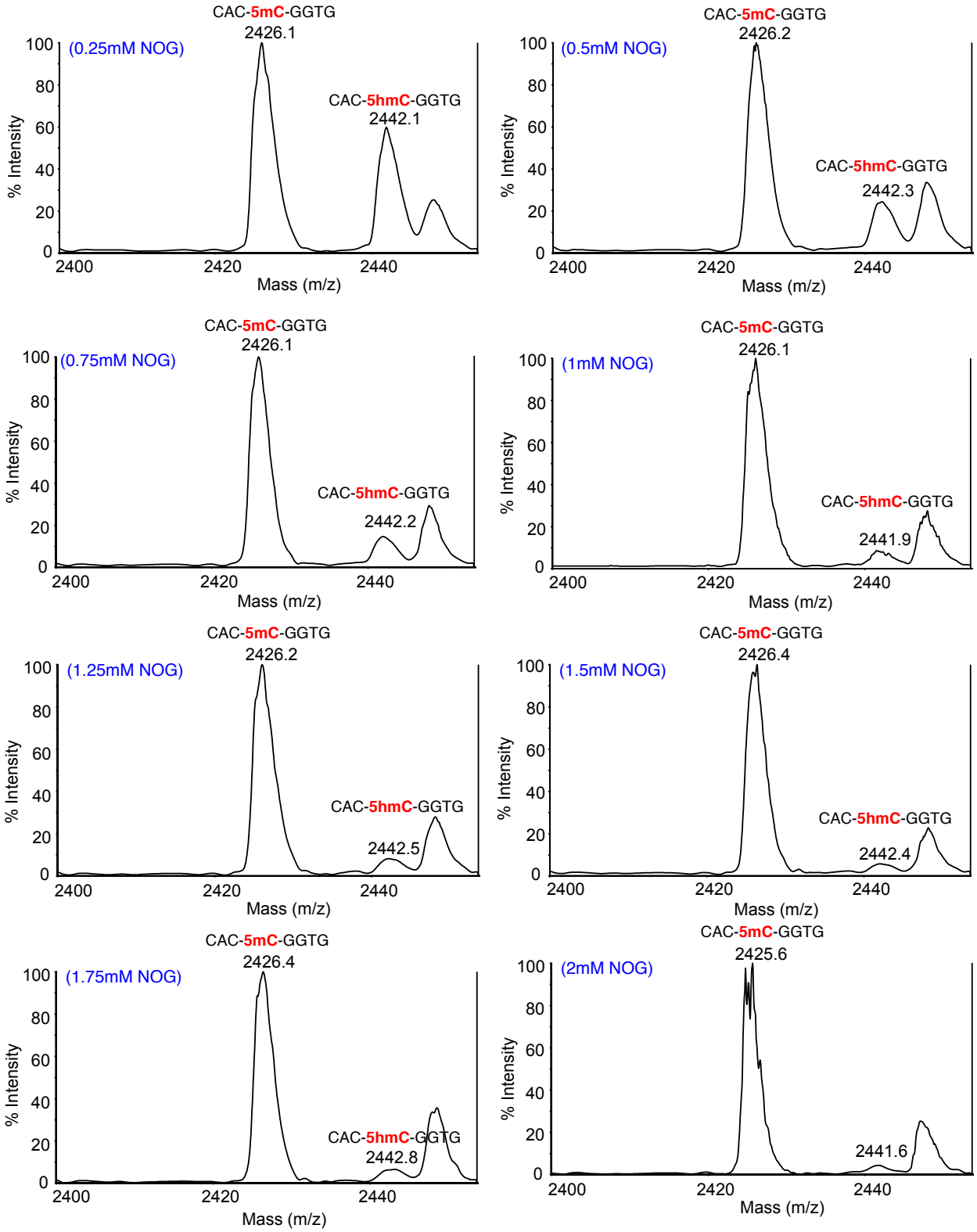

Supplementary Figure S8 continued: NOG concentration-dependent inhibition of TET2 catalytic activity

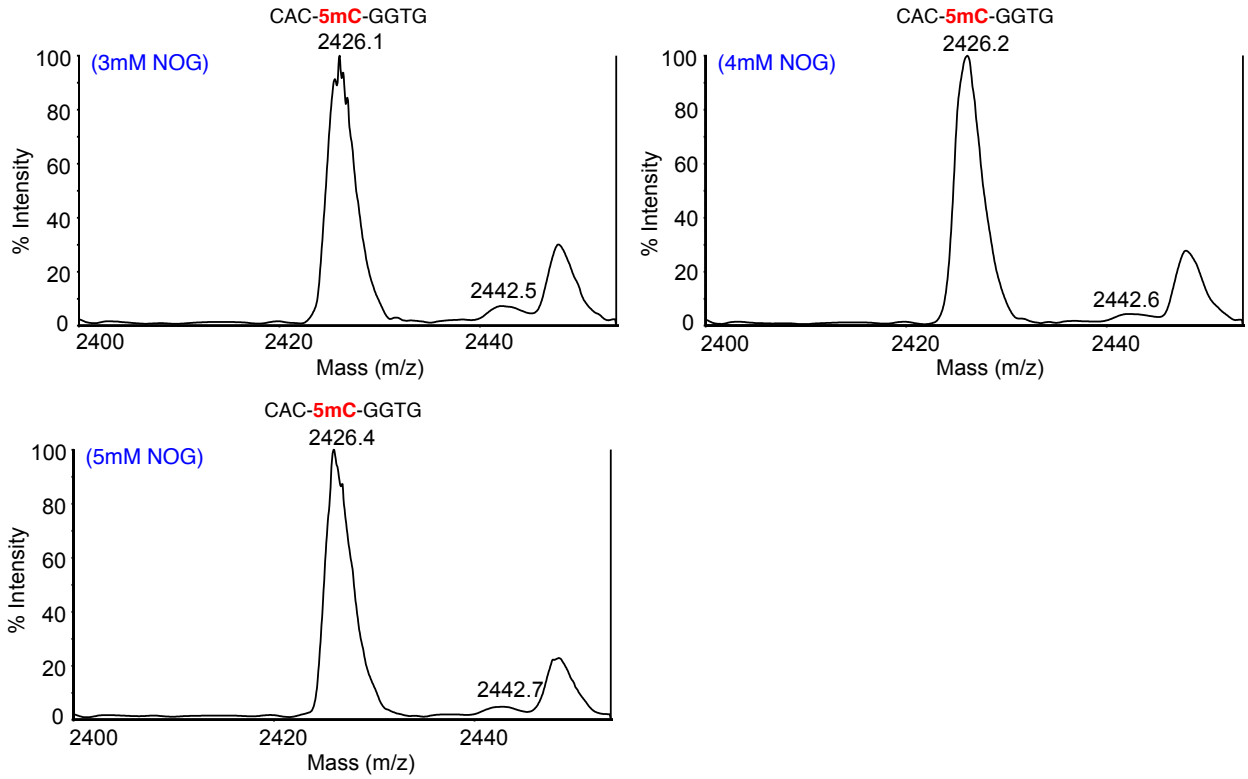

Supplementary Figure S8 continued: NOG concentration-dependent inhibition of TET2 catalytic activity

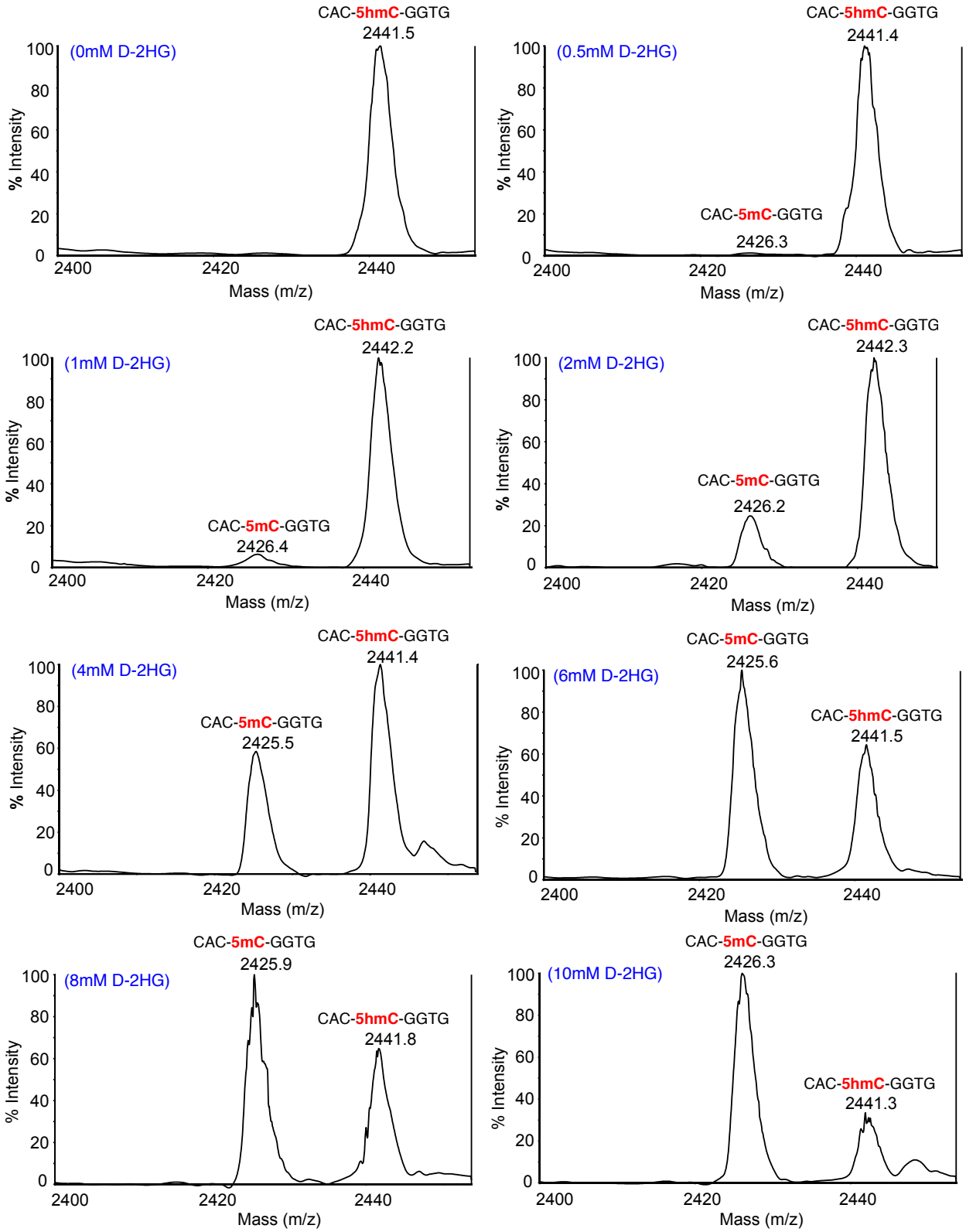

Supplementary Figure S9: D-2HG concentration-dependent inhibition of TET2 catalytic activity

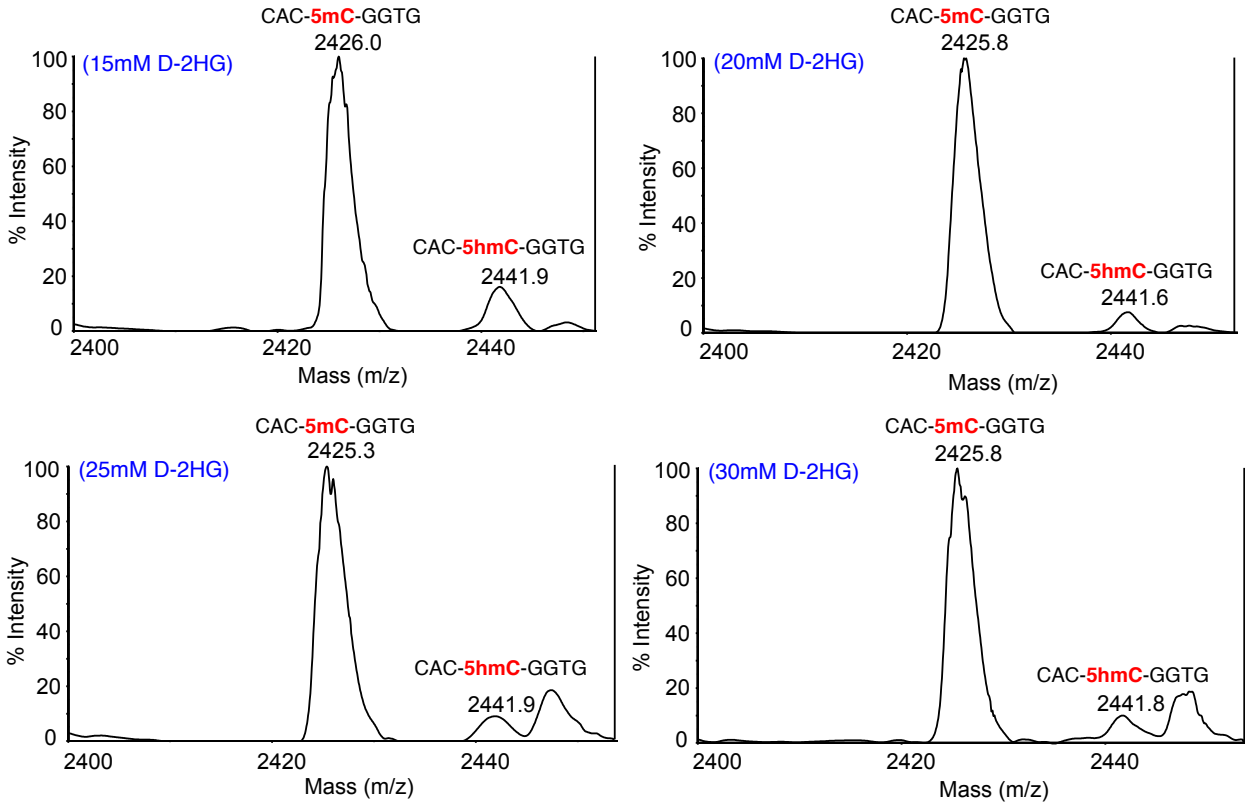

Supplementary Figure S9 continued: D-2HG concentration-dependent inhibition of TET2 catalytic activity

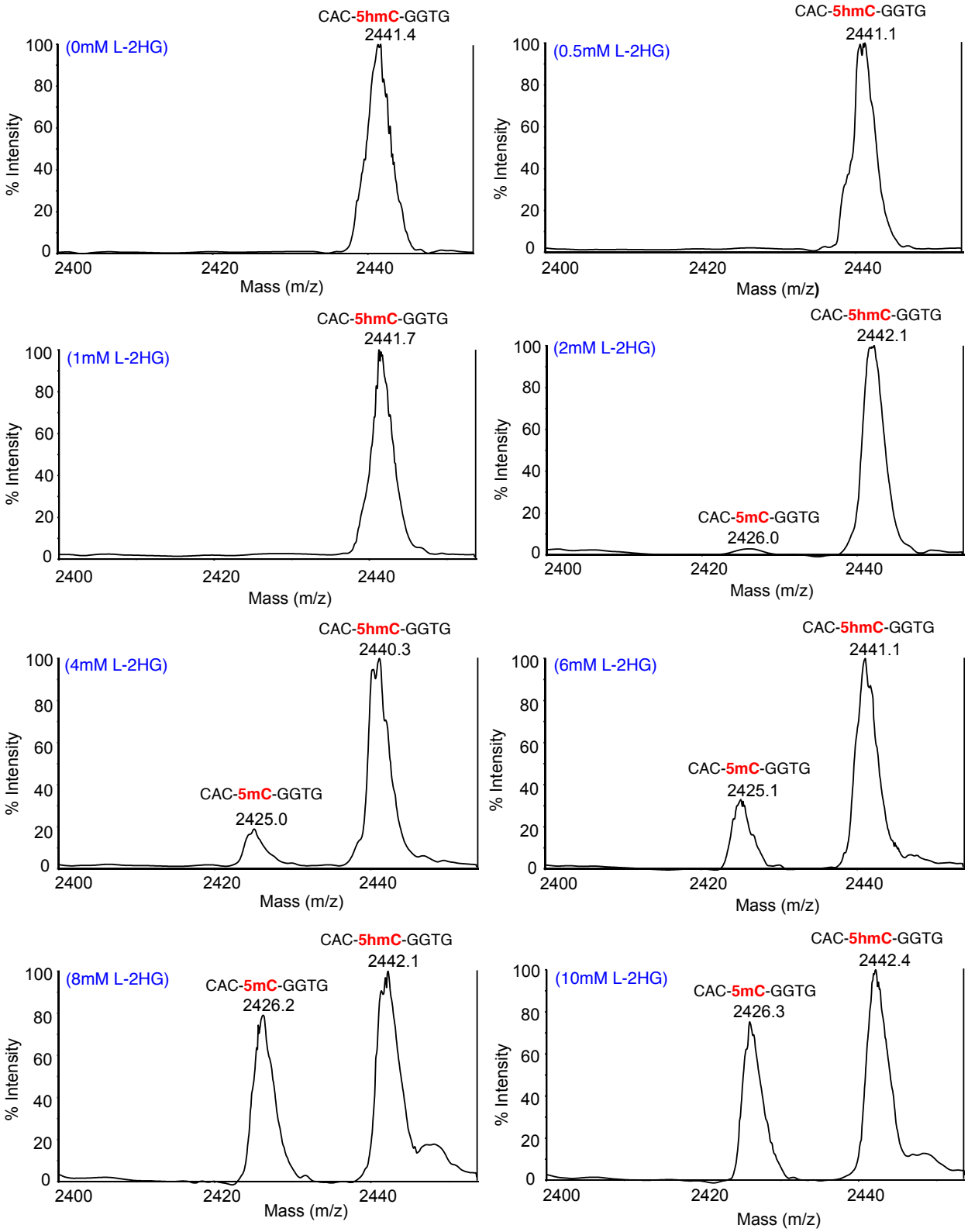

Supplementary Figure S10: L-2HG concentration-dependent inhibition of TET2 catalytic activity

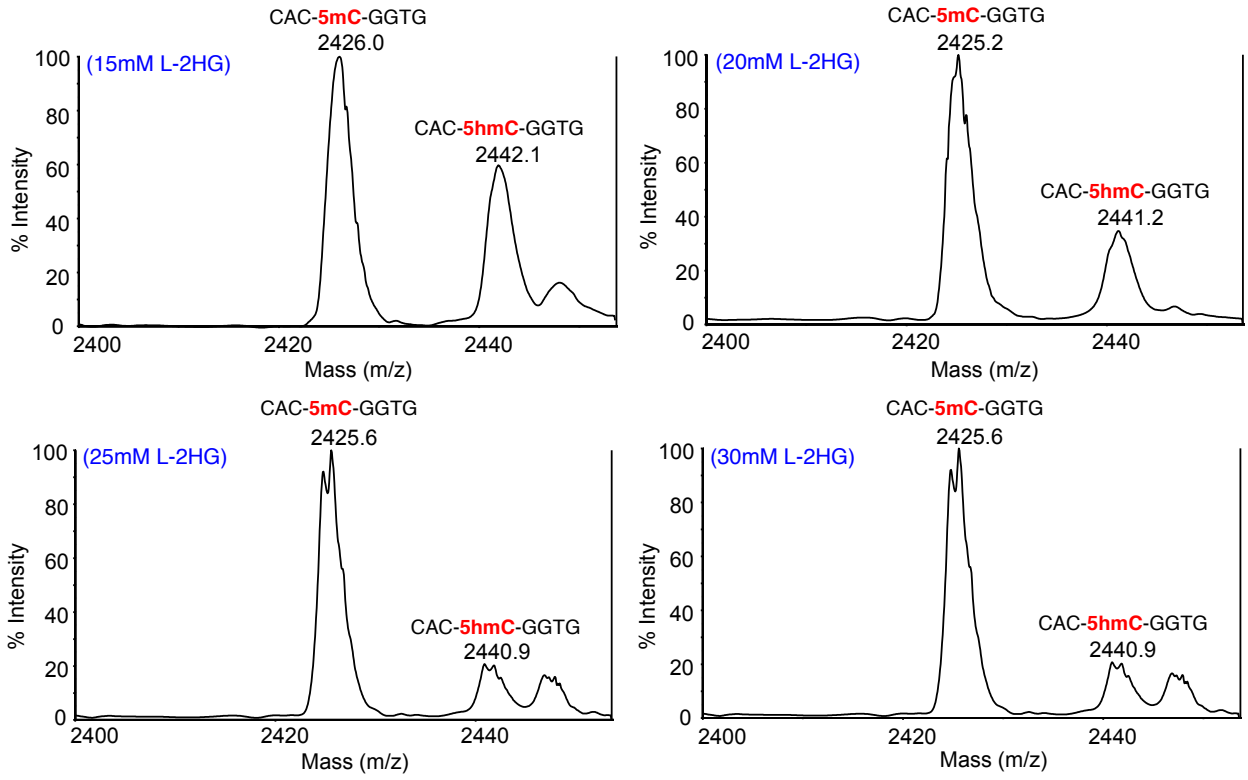

Supplementary Figure S10 continued: L-2HG concentration-dependent inhibition of TET2 catalytic activity